18

Electromagnetic Wave Absorption Properties of Nanoscaled ZnO

Yue Zhang, Yunhua Huang and Huifeng Li
University of Science and Technology Beijing
China

1. Introduction

Microwave absorbing material (MAM) is a kind of functional material that can absorb electromagnetic wave effectively and convert electromagnetic energy into heat or make electromagnetic wave disappear by interference (Kimura et al., 2007). MAM is currently gaining much attention in the field of civil and military applications. For example, the materials have been widely applied to minimize the reflection of microwave darkrooms, airplanes, steamboats, tanks and so on (Zou et al., 2008). Generally, the electromagnetic absorbing performance of any MAM is linked to its intrinsic electromagnetic properties (i.e. conductivity, complex permittivity and permeability) as well as to extrinsic properties such as the thickness and working frequencies. It is clear that the microwave absorption properties can be improved by changing the above parameters. However, the traditional MAMs or novel nanomaterials still have some disadvantages such as high density, narrow band, and low absorptivity (Zou et al., 2006). Therefore, demands for developing more economical MAMs with "low density, wide band, thin thickness, and high absorptivity" are ever increasing.

Wurtzite-structured ZnO is of great importance for its versatile applications in optoelectronics, piezoelectricity, electromagnetic wave absorption, laser, acous-optical divices, sensors, and so on (Wang et al., 2007). One-dimensional nanostructures of ZnO, such as nanowires, nanobelts, and nanotetrapods, have been a hot research topic in nanotechnology for their unique properties and potential applications. Moreover, several types of three-dimensional ZnO nanostructures have been synthesized. Because of the high surface/volume ratio and integrated platform, three-dimensional oxide networks have been demonstrated for building ultrasensitive and highly selective gas sensors and optoelectronics applications (Zhu et al., 2007). It is worth mentioning that the ZnO nanostructures have shown great attraction for microwave radiation absorption and shielding material in the high-frequency range due to their many unique chemical and physical properties (Zhuo et al., 2008). Some research works focused on nanoscaled ZnO as a vivid microwave absorption material due to their light weight, high surface/volume ratio, and semiconductive and piezoelectric properties (Wang & Song, 2008).

On the other hand, carbon nanotubes (CNTs) as conductive filler have been widely studied in MAMs due to the unique spiral and tubular structure since the discovery of CNTs by Iijima in 1991 (Iijima, 1991). CNTs/polymer composites exhibit a strong microwave absorption in the frequency range of 2-18 GHz and have the potential application as broad

frequency radar absorbing materials (Fan et al., 2006). For example, Zhao et al. demonstrate that carbon nanocoils are chiral microwave absorbing materials and exhibit superior microwave absorption (Zhao & Shen, 2008). However, there are few reports concerning electromagnetic wave absorption properties of ZnO and CNTs nanostructures composites. Furthermore, the nanocrystalline structure of tetraleg ZnO (T-ZnO) is constituted of a central part and four needle-like legs, and exhibits super high strength, wear resistance, vibration insulation and can be widely applied as MAMs (Dai et al, 2002). So, it is necessary to study the absorption properties of T-ZnO and CNTs nanostructures composites.

In this chapter, we will report the synthesis methods of T-ZnO nanomatrials and ZnO micro-/nanorod networks, the fabrication methods of wave absorption coatings using T-ZnO and T-ZnO plus multi-walled CNTs as absorbent respectively, the measurement of wave absorption properties of coatings, the effects of absorbent contents, thickness of coatings on the properties, the measurement of electromagnetic parameters and the calculated properties of T-ZnO and ZnO networks, and the wave absorption mechanisms.

2. Preparation and structure of microwave absorbing materials

The nanoscaled ZnO used for microwave absorbing samples, including tetraleg ZnO nanorods and three-dimensional ZnO micro-/nanorod networks were synthesized in our laboratory. The other materials, multi-walled carbon nanotubes, were purchased from commercial company. The fabrication methods and structures of nanoscaled ZnO, and the structural characterization of CNTs will be presented as follows.

2.1 Fabrication of tetraleg ZnO

The tetraleg ZnO nanorods are the one type of the easy synthesized morphologies through thermal evaporation method. Tetraleg ZnO nanostructures were fabricated by the following procedure. The metal zinc powders (99.9%) with thickness of 1~3 mm were placed in an alumina ceramics boat in a tubular furnace under a constant flow of argon and oxygen, and the fraction of oxygen was 5 ~ 10%. The furnace was kept to 700 ~ 800˚C, i. e. the reaction temperature, for 20~30 minutes. No catalyzer was utilized in all the deposition processes. White fluffy products were obtained. The materials for the wave-absorbing coatings were synthesized and accumulated as above process. The synthesized products were characterized using X-ray diffraction (XRD) (D/MAX-RB) with Cu-Ka radiation, field-emission scanning electron microscopy (FE-SEM) (LEO1530), and transmission electron microscopy (TEM) (HP-800). Figure 1 shows the SEM images of the morphologies of the tetraleg ZnO nanorods. The obtained ZnO nanostructures are of a tetrapod shape having four legs. The image at low magnification shows that uniform T-ZnO nanorods form in high yield (Fig. 1a). No particles are produced. The high-magnified image (Fig. 1b) indicates that the surfaces of nanorods are smooth. The length of legs of T-ZnO nanorods is 2–4μm. Very little secondary growth components are observed. T-ZnO nanorods we obtained are uniform nanorods.

XRD measurements were made on the mass nanorods to assess the overall structure and phase purity. A typical XRD pattern of the T-ZnO nanorods is shown in Fig. 2. The diffraction peaks can be indexed to a wurtzite structure of ZnO with cell constants of a = 0.324 nm and c = 0.519 nm. No diffraction peaks from Zn or other impurities were found in any of the samples.

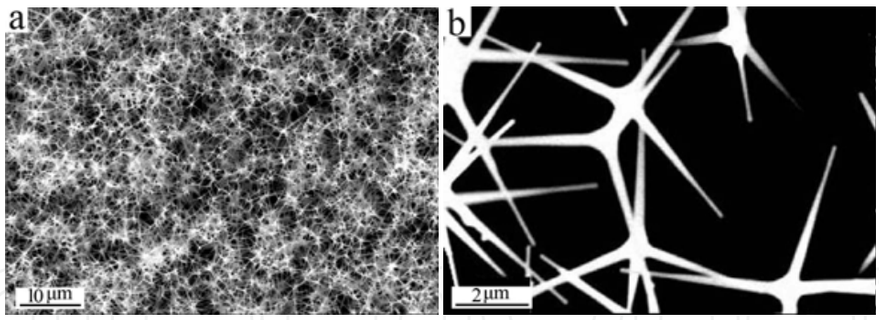

Fig. 1. SEM images of tetraleg ZnO nanorods, (a) Low-magnified, and (b) high-magnified

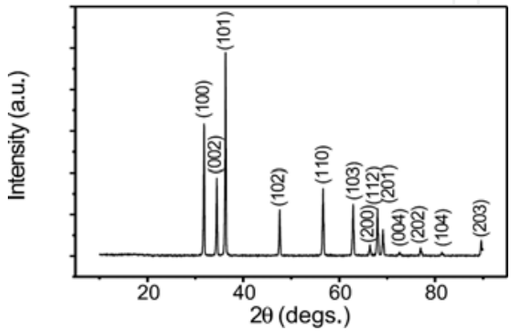

Fig. 2. XRD pattern obtained from a bulk sample of T-ZnO nanorods

HRTEM observation of the T-ZnO nanostructure is shown in Fig. 3. A low-magnification image given in Fig. 3(a) shows the projected four-fold twin structure at the central region. Fig. 3(b) is a corresponding HRTEM image from the central region. It reveals the structure of the twin boundaries between the element crystals. From the HRTEM image, it can be seen that the interfaces are sharp and show no amorphous layer. These twins are smoothly conjugated fairly coherently at the boundaries with little lattice distortion. A Fourier transform of Fig. 3(b) is given in Fig. 3(c), based on which the twin planes can be determined to be the $\{11\ \bar{2}2\}$ family. The index corresponding the grain at the bottom-left corner of Fig. 3(b) is labeled in Fig. 3(c). The twin plane is indicated by an arrowhead. The incident beam direction is $[\ \bar{2}4\ \bar{2}3]$, along which the four twin boundaries are imaged edge-on.

As for the growth mechanism, Iwanaga proposed the octahedral multiple twin (octa-twin) nucleus models (Fujii et al., 1993), and Dai et al. directly revealed the structure of the T-ZnO nanostructures by HRTEM for the first time (Dai et al., 2003). According to the octa-twin nucleus model, ZnO nuclei form in an atmosphere containing oxygen are octa-twins nuclei which consist of eight tetrahedral-shape crystals, each consisting of three $\{11\ \bar{2}\ 2\}$ pyramidal facets and one (0001) basal facet (Fig. 4(a)). The eight tetrahedral crystals are connected together by making the pyramidal faces contacting one with another to form an octahedron. The surfaces of the octa-twin are all basal planes. An important additional condition is that every twin is of the inversion type, i.e. the polarities of the twinned crystals are not mirror-symmetric with respect to the contact plane but antisymmetric. Thus the eight basal surfaces of the octa-twin are alternately the plus (0001) surface (+c) and the minus surface $(000\ \bar{1})$ (-c), as shown in Fig. 4(b). The formation of the tetraleg structure has to do with the following two factors based on the octa-twin nucleus. It is known through the study of ZnO nanowires and nanobelts, [0001] is the fastest growth direction in the formation of

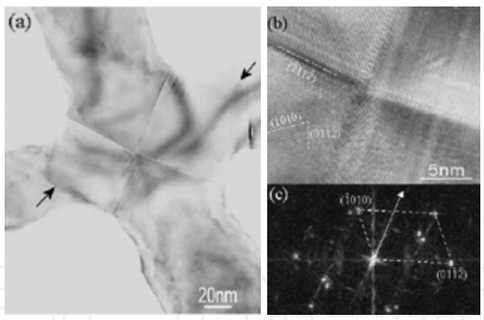

Fig. 3. (a) Low magnification TEM image of a tetraleg ZnO nanostructure. (b) A high-resolution TEM image recorded from the center of the tetraleg structure. (c) A Fourier transform of the image given in (b) and the indexes corresponding to one of the bottom-left grain in (b). The incident beam direction is [$\bar{2}4\ \bar{2}3$]

nanostructure. The octa-twin has four positively charged (0001) surfaces and four negatively charged (0001) surfaces. The positively charged surfaces are likely to be terminated with Zn, which may be the favorable sites to attracting vapor species, resulting in the growth of whiskers along four [0001] directions that have a geometrical configuration analogous to the diamond bonds in diamond. The growth mechanism is believed to be a solid–vapor process.

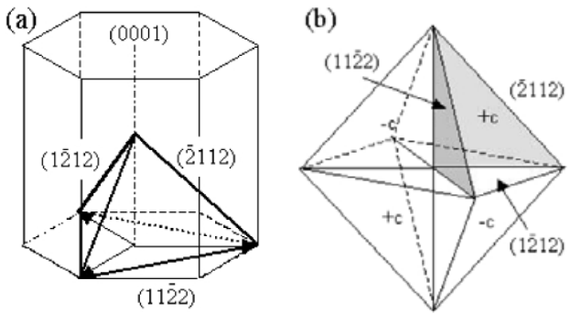

Fig. 4. (a) A pyramid formed by three {11 $\bar{2}$ 2} and one (0001) facets. (b) The octa-twin model composed of eight pyramidal inversion twin crystals

2.2 Fabrication of three-dimensional ZnO networks

The three-dimensional ZnO netlike micro-/nanostructures were fabricated by the following procedure. First, high pure Zn (99.99%) and graphite powders with molar ratio of 10:1 were ground fully into a mixture before being loaded into a quartz boat. The Si substrate with the polished side facing the powder was fixed upon the boat, and the boat with the mixture was placed at the center of the furnace. The vertical distance between the zinc source and the substrate was about 4-6 mm. And then the alumina ceramics boat was inserted into a quartz tube (30 mm inside diameter) of a tubular furnace under a constant flow of argon and oxygen. The flow rate of Argon was 100 standard cubic centimeters per minute (sccm) and the fraction of oxygen was 4 sccm. The quartz tube was heated up to 910 °C, and retain reaction temperature for 30 minutes. After the evaporation finished, a layer of woollike product was formed on the walls of the boat and the surface of the substrate.

The SEM images in Figure 5 show the morphologies of ZnO netlike microstructures. It can be clearly seen that these ZnO micro/nanorods form crossed network, and the rods have the

diameter in the range of 0.2-2μm and the length of 50-100 μm (Fig. 5a). The high magnified image of partial network is shown in Figure1b and the ZnO rods have the diameter of 1-2μm. Also, the Fig. 5b indicates the ZnO microrods with a rough surface, possibly due to the competition between surface energy and strain energy (Li et al., 2010).

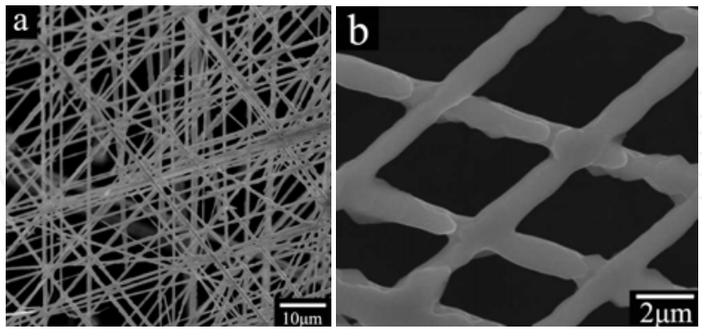

Fig. 5. SEM images of ZnO netlike microstructures, (a) Low-magnified, and (b) high-magnified

In order to obtain more detailed structural information of the ZnO products, typical transmission electron microscopy (TEM) and high-resolution transmission electron microscopy (HRTEM) images were recorded, as shown in Figure 6. Figure 6a reveals a ZnO micro-/nanorods bundle in the 3D networks. The individual ZnO nanorods have the diameters in the range of 200-500 nm and length of several microns. Figure 6b shows the HRTEM image and corresponding SAED pattern taken from the nanorod. The HRTEM image of the fraction in Figure 6b clearly shows the lattice fringes with the d-space of 0.52 nm, which matches that of (0001) planes of the wurtzite structural ZnO. The inset of Figure

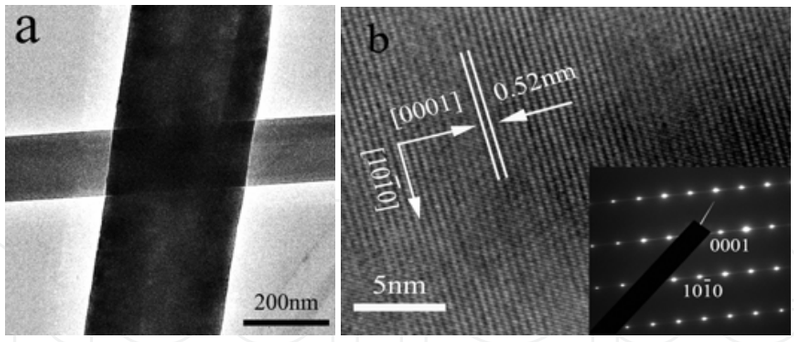

Fig. 6. (a) The low-magnified TEM image of ZnO netlike micro-/nanostructures, (b) the HRTEM image of ZnO netlike micro-/nanostructures, inset: SEAD image of ZnO netlike micro-/nanostructures

6b shows the corresponding SAED pattern taken from the nanorod. Combined HRTEM images with the corresponding SAED pattern, the growth direction of the fraction can be determined along [0001] and [10 $\bar{1}$0]. It is noteworthy that the netlike structures, such as the TEM samples, are sufficiently stable, which cannot be destroyed even after ultrasonication for a long time. Therefore, these electron microscopy characterizations reveal the formation mechanism of ZnO netlike structure is following the V-S mode presented in the literature (Wang et al., 2003).

2.3 Characterization of carbon nanotubes

The multi-walled CNTs were purchased from Beijing Nachen Corporation (Beijing, China), and were observed by a field emission scanning electric microscopy (FE-SEM) (Zeiss, SUPRA-55). The low and high magnified morphologies of the CNTs are shown respectively in figure 7.

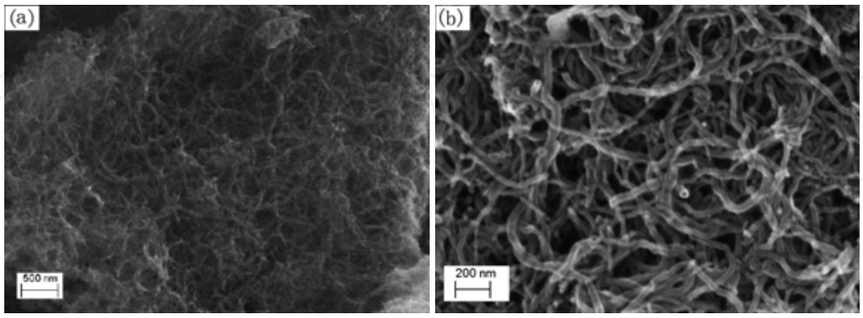

Fig. 7. SEM images of CNTs (a) low-magnified image; (b) high-magnified image

3. Absorption properties of T-ZnO / EP coatings

3.1 Fabrication of T-ZnO / EP coatings

T-ZnO/Epoxy resin (EP) wave-absorbing coatings were fabricated with nanosized T-ZnO as the absorbent and epoxy resin as the binder as follows. The nano T-ZnO was added into the EP resin which was diluted by absolute ethyl alcohol, vibrated by ultrasonic wave for about 1h, and then the curing agent was put into the composite, stirred gently. The mixture was sprayed layer by layer onto aluminum plate with a square of 180mm X 180mm and cured at 25-30°C for at least 2h. The images of the surface and cross-section of the wave-absorbing coating are shown in figure 8 (Cao et al., 2008).

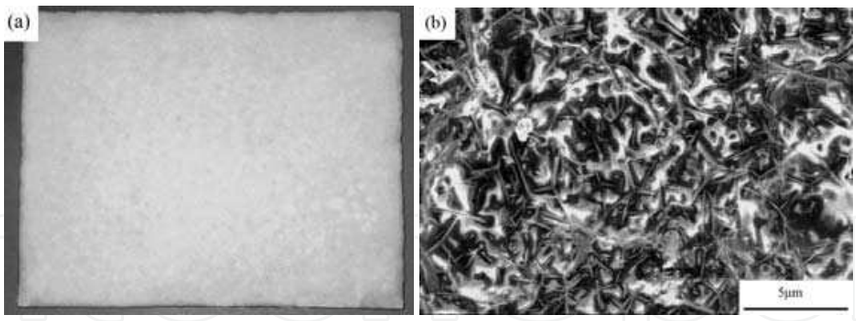

Fig. 8. Images of the cross-section of nano tetraleg ZnO/EP resin coating

The reflectivity of the composites were measured by a reflectivity scanning measurement system (HP 83751B) integrated a signal source (HP 8757E) working at the 2-18 GHz band. The linear scanning frequency was used, and the testing accuracy was better than 0.1 dB. Both the real and imaginary parts of the complex permittivity and permeability of samples were measured by a vector network analyzer system (HP8722ES) in the frequency range of 2-18 GHz. The sample obtained by mixing nanoscaled T-ZnO with molten paraffin was made into a ring of 7.00 / 3.00 × 2.00 mm (outer diameter / inner diameter × thickness) for electromagnetic parameters measurement. The paraffin is transparent for microwave. The details of the measurement system for the microwave absorption properties are shown in Schematic 1.

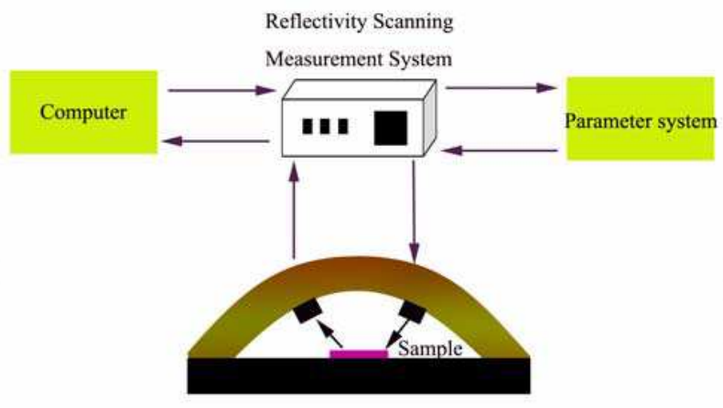

Schem. 1. The schematic of automatic parameter sweep vector network measurement system for measurements the microwave absorption properties

3.2 Microwave absorption properties of T-ZnO / EP coatings

1. **Impacts of concentration of T-ZnO plus CNTs on microwave absorption properties**

The microwave absorption properties of the nano T-ZnO/EP resin coatings with different ZnO concentration and thickness of 1.5 mm are summarized in Table 1. The measurement results, as shown in Fig. 9, reveal that the absorption properties improve as the concentration of nano T-ZnO increases. The minimum reflection loss is -1.74dB when the concentration of nano T-ZnO is 11%, and reduces to -3.23dB, when the content of nano T-ZnO is 16%. The sample A3 with the concentration of 20% shows the minimum reflection loss of -3.89dB at 17.4GHz. The difference on minimum reflection loss of the coatings is associated with the concentration of nano T-ZnO in the coating, which attenuates the electromagnetic wave energy mainly by forming conductive networks.

Sample number	*T-ZnO concentration (wt%)*	*Thickness (mm)*	*Minimum reflection loss (dB)*	*Corresponding frequency (GHz)*
A1	11	1.5	-1.74	15.7
A2	16	1.5	-3.23	18.0
A3	20	1.5	-3.89	17.4

Table 1. Absorption properties of ZnO /EP resin coatings with different ZnO concentration

2. **Impacts of the coating thickness on microwave absorption properties**

In other research, the absorption properties of ZnO /EP resin coatings with different thickness were measured. A list of the microwave absorption properties of the samples is presented in Table 2 and Fig. 10. The results indicate that the absorption properties improve as the coating thickness increases. The minimum reflection loss is -0.38dB when the thickness is 11%, and reduce to -5.30dB, as the thickness is -2.5 dB. When the thickness increases to 3.5mm, the minimum reflection loss reaches to -9.11dB. On the other hand, it can also be seen that the maximum absorbing peak shifts towards a lower frequency as the thickness increases. When the coating thickness enlarges from 1.5mm to 2.5 and 3.5 mm, the peak frequency is 14.0, 12.9 and 8.8 GHz respectively.

Sample number	*T-ZnO concentration (wt%)*	*Thickness (mm)*	*Minimum reflection loss (dB)*	*Corresponding frequency (GHz)*
B1	28.6	1.5	-0.38	14.0
B2	28.6	2.5	-5.30	12.9
B3	28.6	3.5	-9.11	8.8

Table 2. Absorption properties of ZnO /EP resin coatings with different thickness

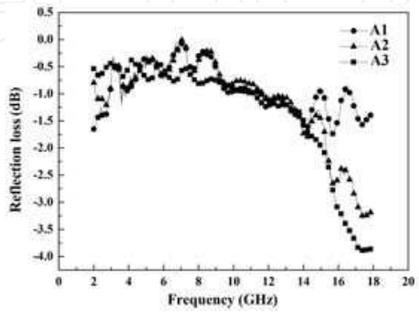

Fig. 9. Absorption characteristics of ZnO/EP resin coatings with different ZnO concentration

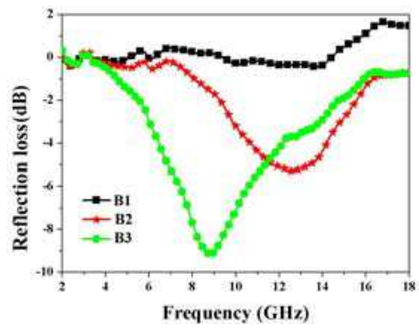

Fig. 10. Absorption characteristics of ZnO/EP resin coatings with different thickness

3. Intrinsic reasons of T-ZnO plus CNTs for microwave absorption

Microwave absorption may result from dielectric loss and/or magnetic loss. They are characterized with the complex relative permittivity ε_r ($\varepsilon_r = \varepsilon' - j\varepsilon''$, where ε' is the real part, ε'' the imaginary part) and the complex relative permeability μ_r ($\mu_r = \mu' - j\mu''$, where $\mu'$is the real part, μ'' the imaginary part) (Zhang et al., 2008).

In order to investigate the intrinsic reasons for microwave absorption of the coating, the complex permittivity ε and permeability μ of the nano T-ZnO were measured. Fig.11a and Fig.11b show the frequency dependence of the permittivity and permeability of nano T-ZnO, respectively. From the figures, it is found that the values of imaginary part of permittivity of T-ZnO nanorods are larger than that of permeability of T-ZnO nanorods, the value of imaginary part of permittivity and permeability are getting close to 3.0 and 1.0, respectively. The results revealed that the value of dielectric loss $\tan\delta_E$ ($\varepsilon''/\varepsilon'$) is larger than that of magnetic loss $\tan\delta_M$ (μ''/μ'). Thus, the electromagnetic wave absorptions of T-ZnO nanorods are mainly caused by dielectric loss rather than magnetic loss.

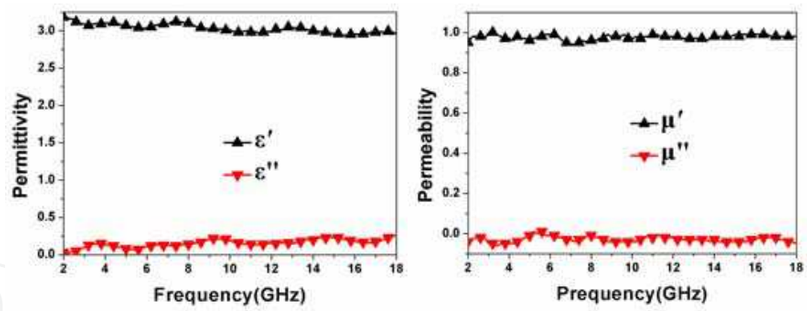

Fig. 11. Frequency dependence of the permittivity (a) and permeability (b) of tetraleg ZnO

From the above analysis, the wave-absorbing mechanism can be derivated. Firstly, the diameter of needle-body of nano T-ZnO belongs to the nanoscale range, so the quantum confine effect makes the wave-absorbing properties of nano T-ZnO change greatly. According to the Kubo theory, the energy levels in nano T-ZnO are not continuous but split because of the quantum confine effect. When an energy level is in the range of microwave energy, the electron will absorb a photon to hop from a low energy level to a higher one. Also, the defects and suspending band can cause multiple scattering and interface polarization, which result in the electromagnetic wave absorption. Secondly, the wavelength of 2~18GHz electromagnetic wave is lager than the size of nano T-ZnO, which can reduce the electromagnetic wave reflection. It can easily lead to Rayleigh scattering when the incident electromagnetic wave reacts with the nano T-ZnO, which results in the electromagnetic wave absorption in all direction. Furthermore, it can be found that the coating is constituted of networks resulted from the tetraleg-shaped structure of nano T-ZnO, and nano T-ZnO have good conductive property in comparison with the common oxides, so it is available for the electromagnetic wave to penetrate the cellular material formed by the numerous conductive networks of nano T-ZnO and the energy will be induced into dissipative current, which leads to the energy attenuation. The earlier analysis of the related system indicates that the charge concentration at the needles' tip of the T-ZnO is distinct when the material is under an electric field because of the larger aspect ratio and the limited conductivity of the nano T-ZnO. So, it is reasonable that the concentrated tips will act as multipoles that will be tuned with the incident electromagnetic waves and contributes to strong absorption (Zhou et al., 2003). Besides above, the piezoelectric character of nano T-ZnO is also a factor of damaging the entered energy of microwave and reducing the reflectivity.

4. Absorption properties of T-ZnO plus CNTs / EP coatings

4.1 Fabrication of T-ZnO plus CNTs / EP coatings

As the multi-walled CNTs and T-ZnO nanostructures were prepared, the typical fabrication process of CNT/T-ZnO/EP composites is as follows. The calculated amount of mixed raw CNTs and T-ZnO nanostructures were sufficiently dispersed by ultrasonication for about 30 minutes. Then the mixture was added into EP, which was diluted by absolute ethyl alcohol, and dispersed by ultrasonication for about 30 minutes again, and then the curing agent was put into the composites, stirred gently. The mixture was sprayed layer by layer onto an aluminum plate with a square of 180 mm × 180 mm and cured at room temperature for at least 24 hours. Considering the preparing conditions, the thickness error of the epoxy

composites was controlled to ± 0.1 mm. The measurement results are same within the range of the system measurement error range. A list of the microwave absorption properties of all manufactured samples is presented in Table 3. There are three samples of the same lot which have been prepared and tested, and we have obtained the average data of three samples to examine their absorption properties.

The morphologies of absorbents and CNTs/T-ZnO/EP composites were also observed by a FE-SEM (Zeiss, SUPRA-55), as shown in figure 12.

The measurements of reflectivity of the composites, complex permittivity and permeability of samples, and the measurement system refer to part 3.1. The sample was made by mixing nanoscaled T-ZnO/CNTs with molten paraffin into a ring for electromagnetic parameters measurement.

Sample Number	*CNT concentration (wt%)*	*T-ZnO concentration (wt%)*	*Thickness (mm)*	*Minimum reflection loss (dB)*	*Corresponding frequency (GHz)*	*Absorption bandwidth (<10GHz) (GHz)*
1 #	0	20	1.2±0.1	-3.48	10.24	0
2#	8	0	1.2±0.1	-7.83	18.00	0
3#	12	0	1.2±0.1	-9.35	18.00	0
4 #	20	0	1.2±0.1	-8.48	17.78	0
5 #	8	12	1.2±0.1	-11.21	16.16	1.5
6 #	12	8	1.2±0.1	-13.36	14.24	2.8
7 #	12	8	1.5±0.1	-23.07	12.16	5
8 #	12	8	2.2±0.1	-23.23	12.8	4.4
9 #	12	8	2.7±0.1	-19.95	8.16	2.56

Table 3. Microwave absorption properties of prepared CNTs/T-ZnO/EP composites

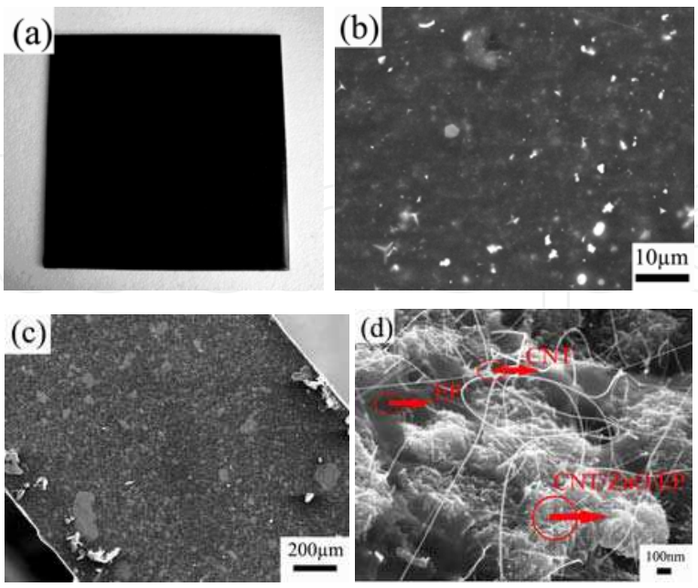

Fig. 12. Typical SEM images of CNTs/T-ZnO /EP composites: (a) and (b) coating surface; (c) and (d) fractured cross-section.

4.2 Microwave absorption properties of T-ZnO plus CNTs / EP coatings

1. **Impacts of concentration of T-ZnO plus CNTs on microwave absorption properties**

In order to investigate the impacts of concentration of CNTs and T-ZnO nanostructures on microwave absorption properties, the absorption properties of CNTs/T-ZnO/EP composites with thickness of 1.2 mm were measured as shown in Fig. 13 (Li et al., 2010). It can be seen that CNTs and T-ZnO nanostructures concentration has an obvious effect on microwave absorption properties. T-ZnO/EP and CNTs/EP composites have weak absorption performance. The value of the minimum reflection loss for T-ZnO/EP composite corresponding to sample 1# is -3.48 dB at 10.24 GHz, and for CNTs/EP composite corresponding to sample 2#, 3# and 4#, the value of the minimum reflection loss are -7.83 dB at 18.00 GHz, -9.35 dB at 18.00 GHz, and -8.48 dB at 17.78 GHz, respectively. CNTs/T-ZnO/EP composites corresponding to sample 5# achieve a maximum absorbing value of -11.21 dB at 16.16 GHz , and reflection loss is over 10 dB (90% absorption) between 15.52 GHz and 17.04 GHz, when the content of CNTs and T-ZnO nanostructures are 8 wt% and 12 wt%, respectively. The maximum absorption for CNTs/T-ZnO/EP composite corresponding to sample 6# reaches 13.36 dB at 14.24 GHz, and the reflection loss is over 10 dB between 13.28 GHz and 16 GHz, when the content of CNTs increases to 12 wt% and T-ZnO nanostructures decreases to 8 wt%, respectively. The curves indicate that the CNTs mixed with an appropriate amount of T-ZnO nanostructures can optimize the absorbent impedance matching and attenuation characteristics (Yusoff et al., 2002). The microwave absorption properties of CNTs/T-ZnO/EP composites are improved significantly with the content of CNTs and T-ZnO nanostructures being 12 wt% and 8 wt%, respectively. It is clear that the positions of microwave absorption peaks move towards the lower frequencies due to the increase of T-ZnO nanostructures amount. The result is similar to the previous report on CNTs/Ag-NWs coatings [19], which shows that the positions of microwave absorption peaks move towards the lower frequencies by filling the Ag nanowires into multi-walled CNTs. This indicates that the absorption peak frequency of the CNTs/T-ZnO/EP composites can be modulated easily by changing the amount of CNTs and T-ZnO nanostructures (Fan et al., 2006).

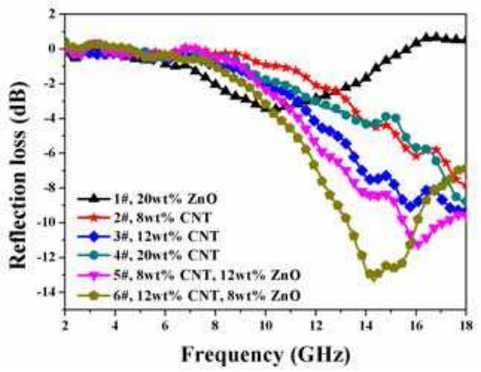

Fig. 13. Absorption properties of CNTs/T-ZnO/EP composites with different CNT and T-ZnO nanostructure content

About the mechanism of the CNTs/T-ZnO/EP, we think that the nanostructures of T-ZnO possess isotropic crystal symmetry play an important role in the process of microwave absorption. It can form isotropic quasiantennas and some incontinuous networks in the composites. Then, it is available for the electromagnetic wave to penetrate the

nanocomposites formed by the numerous antenna-like semiconductive T-ZnO nanostructures and the energy will be induced into a dissipative current, and then the current will be consumed in the incontinuous networks, which lead to the energy attenuation [14, 15]. On the other hand, there are many interfaces between the epoxy matrix and CNTs outer surfaces. Compared with the CNTs, there are more interfaces between the T-ZnO and CNTs inner surfaces in the composites. Therefore, interfacial multipoles contribute to the absorption of the CNT/T-ZnO/EP composites (Zhao et al., 2008). These results were confirmed the Cao et al. by the theoretical calculation (Fang et al., 2010). Furthermore, the size, defects, and impurities also have effects on the microwave absorption property of the T-ZnO.

2. **Impacts of the coating thickness on microwave absorption properties**

To further study the influence of the composite thickness on microwave absorption properties, CNTs/T-ZnO/EP composites with various thickness were prepared by fixing CNTs and T-ZnO content of 12 wt% and 8 wt%, respectively. Figure 14(a) shows that the value of the minimum reflection loss for CNTs/T-ZnO/EP composite corresponding to sample 6# is -13.36 dB at 14.24 GHz with a thickness of 1.2 mm, and the bandwidth corresponding to reflection loss below -10 dB is 2.8 GHz. When the thickness of CNTs/T-ZnO/EP composite corresponding to sample 7# is 1.5 mm, the microwave absorption properties have been improved obviously. The value of the minimum reflection loss for CNTs/T-ZnO/EP composite is -23.00 dB at 12.16 GHz, and the bandwidth corresponding to reflection loss below -10 dB is 5 GHz (from 10.60 GHz to 15.60 GHz). Continuing to increase the thickness to 2.2 mm, the microwave absorption properties have little change. The value of the minimum reflection loss for CNTs/T-ZnO/EP composite corresponding to sample 8# is -23.24 dB at 12.71 GHz, and the bandwidth corresponding to the reflection loss below -10 dB is 4.4 GHz. When composite thickness increases to 2.7 mm, the value of the minimum reflection loss for CNTs/T-ZnO/EP composite corresponding to sample 9# is -19.95 dB at 8.16 GHz, the bandwidth correspondingly is 2.56 GHz. It can also be seen that the maximum absorbing peaks shift towards a lower frequency with the increase of composite thickness, which is due to the interference resonance vibration caused by electromagnetic wave and the coating (Zhang et al., 2008).

To clarify the impact of composite thickness on microwave absorption properties, we plotted a curve about the frequency dependence of absorption bandwidth and thickness of CNTs/T-ZnO/EP composites, as shown in Fig. 14(b). The frequency bandwidth of CNTs/T-ZnO/EP composites initially increases, and then decreases with the increase of the composite thickness. When the thickness is up to 1.5mm, the frequency bandwidth reaches the maximum value of 5 GHz. This indicates that the CNTs mixed with T-ZnO nanostructures have potential application as the broad frequency absorbing materials.

3. **Intrinsic reasons of T-ZnO plus CNTs for microwave absorption**

In order to investigate the intrinsic reasons for microwave absorption of CNTs and T-ZnO nanostructures composites, the complex permittivity and permeability of the studied samples were measured. The preparation of the samples can be seen in the experimental part. As CNTs and T-ZnO nanostructures are dielectric absorbents, the real and imaginary parts of the complex permittivity are shown in Fig. 15. Compared with nanoscaled CNTs and T-ZnO/CNTs composites, it is apparent that both the real and imaginary parts of the complex permittivity of T-ZnO nanostructures are greatly smaller. The tangent loss of permittivity of nanoscaled T-ZnO/CNTs are shown in Fig. 16. It can be seen that the values of tangent loss of permittivity of nanoscaled T-ZnO/CNTs are sensitive to the content of

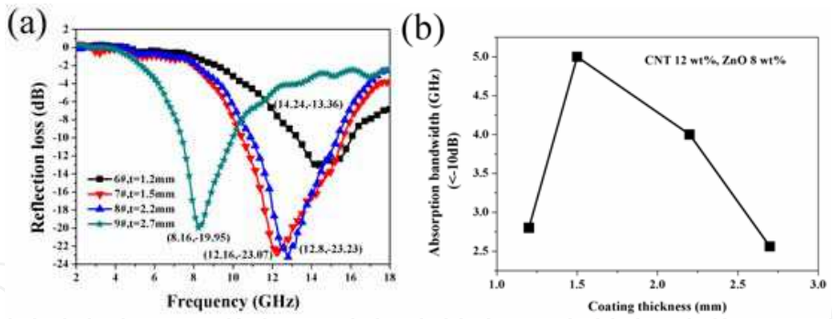

Fig. 14. (a) Absorption properties of CNTs/T-ZnO/EP composites with different thickness; (b) Frequency dependence of absorption bandwidth and coating thickness of CNTs/T-ZnO/EP composites

CNTs. The larger the CNTs mass fraction, the higher are the tangent loss constant. The sample with 20 wt% CNTs has the largest values. There is an obvious peak at 13 GHz for the sample with 12 wt% CNTs and 8 wt% T-ZnO nanostructures. So we calculated the reflection loss of 20% CNTs and 12% CNTs mixed with 8% T-ZnO nanostructures at different thickness as shown in Fig. 17. It is apparent that 12% CNTs mixed with 8% T-ZnO nanostructures gives the optimum microwave absorption. The minimum reflection loss is -12.20 dB at 17.2 GHz with 1.2 mm thickness. The maximum bandwidth under -5 dB (68% absorption) is 6.7 GHz with 1.5 mm thickness, which is consistent with the experimental results as shown in Fig. 14. The experiment and calculation results indicate that CNTs mixed T-ZnO nanostructures have excellent absorption property.

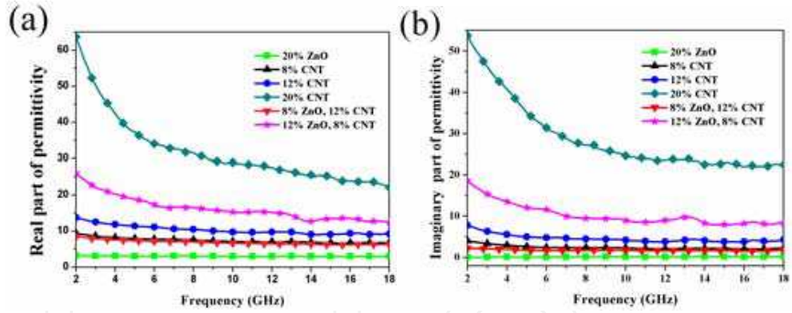

Fig. 15. Frequency dependence of complex permittivity: (a) the real part of permittivity; (b) the imaginary part of permittivity

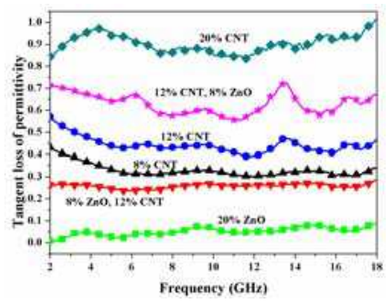

Fig. 16. Tangent loss of permittivity

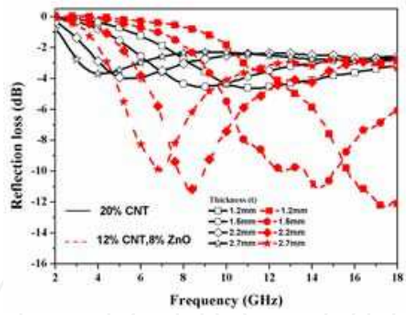

Fig. 17. Calculation of reflection loss of 20% and 12% CNTs mixed with 8% T-ZnO at different thickness

According to the results mentioned above, CNTs/T-ZnO/EP composites exhibit excellent microwave absorption properties compared with that of CNTs/EP and T-ZnO/EP composites. A continuous network formed by a small number of CNTs and some discontinuous networks formed by T-ZnO nanostructures coexist together with CNTs and EP in the composites. This special morphology is available for the electromagnetic wave to penetrate the composites and the energy will be induced into a dissipative current, and then the current will be consumed in the discontinuous networks, which leads to energy attenuation (Zhuo et al., 2008). More importantly, the microwave absorption of CNTs/T-ZnO/EP composites is attributed to interfacial electric polarization. The multi-interfaces between CNTs, T-ZnO nanostructures, EP and lots of agglomerates can be benefit for the microwave absorption because of the interactions of electromagnetic radiation with charge multipoles at the interface (Fang et al., 2010).

5. Absorption properties of three-dimensional ZnO micro-/nanorod networks

Both three-dimensional netlikes ZnO and T-ZnO composite samples used for microwave absorption measurement were prepared by mixing the ZnO netlike micro-/nanostructures and the T-ZnO with paraffin wax with 50 vol % of the ZnO, respectively. The composite samples were then pressed into cylindrical-shaped compact (φ_{out}: 7.00 mm; φ_{in}: 3.04 mm) for the tests of the complex permittivity ε and permeability μ. The measurement system and method are the same as part 3.1.

To investigate the microwave absorption property of netlike ZnO micro-/nanostructures, the complex permittivity ε of the netlike micro-/nanostructures was measured. For comparison, T-ZnO structures were corresponding studied. Figure 18 shows the plots of the frequency versus the complex permittivity of the primary ZnO netlike micro-/nanostructures composites with 50 vol % ZnO netlike nanostructures (SEM image shown in the insert of Fig. 18a) and T-ZnO composites with 50 vol % T-ZnO (See the insert in Fig. 18b). The real permittivity of T-ZnO composite is about 3.1, and the imaginary permittivity is about 0.2 (corresponding green curve). However, for the ZnO netlike micro-/nanostructures composite, the ε′ and ε″ values show a complex variation (corresponding red curve). The real part of relative permittivity (ε′) declines from 15 to 6 in the frequency range of 2-18 GHz (Fig. 18a). The imaginary part of permittivity (ε″) decreases from 4.4 to 3.6 and the curve exhibits two broad peaks in the 7-9 and 12-15 GHz ranges (Fig. 18b). It is worthy to notice that the peaks of the ε″ curve appear at 8 and 14 GHz, suggesting a resonance behavior, which is expected when the composite is highly conductive and skin effect becomes significant. The imaginary part ε″ of ZnO netlike micro-/nanostructures is

relatively higher in contrast to that of T-ZnO composites, which implies the distinct dielectric loss properties arising from the morphology variation. It is reasonable that the dielectric loss is attributed to the lags of polarization between the 3D frame interfaces as the frequency is varied. ZnO netlike micro-/nanostructures possess more complicated interfaces than T-ZnO, resulting in better dielectric loss properties (Zhuo et al., 2008).

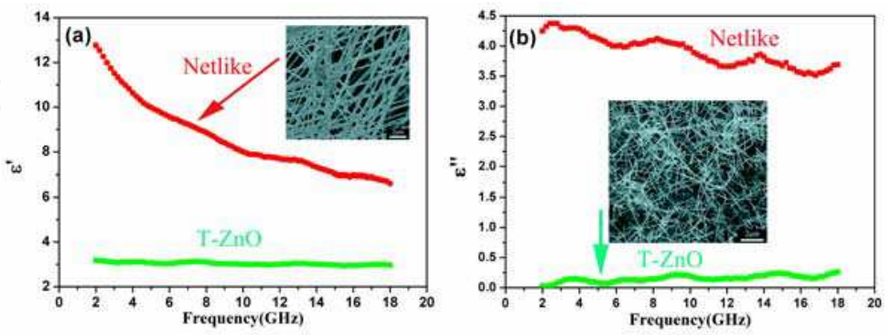

Fig. 18. The frequency dependence of (a) real ε′ and (b) imaginary ε″ parts of relative complex permittivity for ZnO nanotetrapod composite and netlike structures composite. The SEM image of ZnO netlike micro-/nanostructures and T-ZnO nanostructures insert in Fig.4a and Fig.4b, respectively

To explain the microwave absorption properties of the samples measured above, the reflection loss (RL) of the netlike micro-/nanostructures and T-ZnO were calculated, respectively, using the relative complex permeability and permittivity at a given frequency and thickness layer according to the transmit-line theory, which follows the equations below (Sun et al., 2009):

$$Z_{in} = Z_0(\mu_r/\varepsilon)^{1/2}\tanh[j(2\pi fd/c)(\mu_r\varepsilon)^{1/2}] \quad (1)$$

$$RL(dB) = 20\log|(Z_{in}-Z_0)/(Z_{in}+Z_0)| \quad (2)$$

where, f is the microwave frequency, d is the thickness of the absorber, c is the velocity of light, Z_0 is the impedance of air and Z_{in} is the input impedance of the absorber. The relative complex permeability and permittivity were tested on a network analyzer in the range 2-18 GHz. The simulations of the reflection loss of the two composites with a thickness of 2.0 mm are shown in Figure 19a. The ZnO netlike micro-/nanostructures composite possesses a strong microwave absorption property, the value of the minimum reflection loss for the composite is -30 dB at 14.4 GHz. However, the T-ZnO composite almost has no absorption. Figure 19b shows simulations of reflection loss of ZnO netlike micro-/nanostructures composite with different thicknesses. The value of the minimum reflection loss for the ZnO netlike micro-/nanostructures composite is -37 dB at 6.2 GHz with a thickness of 4.0 mm. Compared with the previous report, (Zhuo et al., 2008) in which the value of minimum reflection loss for the composite with 50 vol % ZnO dendritic nanostructures is -25dB at 4.2 GHz with a thickness of 4.0 mm, the ZnO netlike micro-/nanostructures have more excellent properties.

About the mechanism of microwave absorption, P. X. Yan et al. explained the ZnO nanotrees microwaves absorption performances using isotropic antenna mechanism. The random distribution of the isotropic quasi-antenna ZnO semiconductive crystals not only leads to diffuse scattering of the incident microwaves, which results in the attenuation of electromagnetic (EM) energy, but also acts as receivers of microwaves, which can produce

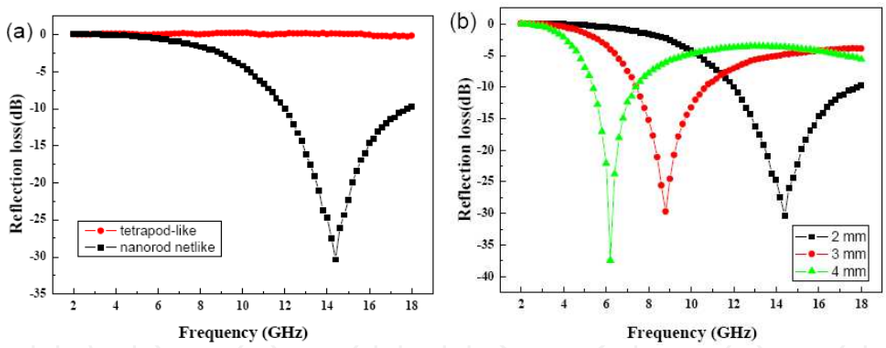

Fig. 19. (a) Simulation of reflection loss of 50 vol % ZnO nanotetrapod and 50 vol % ZnO netlike micro-/nanostructures composites with a thickness of 2.0 mm. (b) Simulation of reflection loss of 50 vol % ZnO netlikes micro-/nanostructures composite with different thickness

vibrating microcurrent in the local networks. Here, in our experiment, we noted that the ZnO netlike structures have special geometrical morphology. Such isotropic crystal symmetry can form continuous isotropic antennas networks in the composites. Moreover, it is available for the EM wave to penetrate the nanocomposites formed by the numerous conductive ZnO networks, and the energy will be induced into dissipative current by random distributed isotropic antennas, and then part of the current will generate EM radiation and the rest will be consumed in the discontinuous networks, which lead to the energy attenuation. Thus, the tanglesome network frame of ZnO nanostructures in the composite will induce a certain extent of conductive loss. Compared with ZnO netlike micro-/nanostructures, no complex frame exists in T-ZnO with the quasi-One-dimensional nanostructures as same as nanowire. A large part of EM radiation will counteract with each other when the orientation of these isotropic quasi-antennas distributes randomly. In a word, ZnO netlike nanostructures, acting as receiving antenna, can receive EM energy and transform it into dissipative current. And they also act as sending antenna transforming the vibrating current into EM radiation. Besides these, the interfacial electric polarization should also be considered. The multi-interfaces between isotropic antenna frame, and air bubbles can benefit for the microwave absorption because of the interactions of EM radiation with charged multipoles at the interfaces (Chen et al., 2004 & Zhuo et al., 2008).

6. Conclusion

1. The effective absorption of T-ZnO/ EP coatings is distributed in the wave band from 15GHz to 18GHz when the content of ZnO is 11-20 wt% and the coating thickness is 1.5mm. As the content of ZnO and the coating thickness increase to 28.6 wt% and 3.5mm, the absorption properties of the coatings improve significantly, especially in the wave band from 6GHz to 12GHz. The minimum reflection loss value is -9.11 dB at 8.80 GHz, and the bandwidth is 4.6 GHz as the reflection loss reaches below -5 dB.
2. For CNTs/ T-ZnO/ EP composite coatings, when the content of CNTs and T-ZnO nanostructures are 12 wt% and 8 wt%, respectively, and the coating thickness is 1.5 mm, the minimum reflection loss of CNTs/ T-ZnO/ EP coatings is -23.00 dB at 12.16 GHz, and the bandwidth corresponding to reflection loss below -5 dB is 7.8 GHz.
3. Both T-ZnO/ EP coatings and CNTs/ T-ZnO/ EP composite coatings have the potential applications in electromagnetic wave shielding, but the CNTs/ T-ZnO composites used

as the microwave absorbents are more effective in the conditions of the thin and light shielding coatings.

4. On the other hand, according to the complex permittivity and the reflection loss simulations of T-ZnO and ZnO networks used as the absorbent in the coatings with the ZnO proportion of 50 vol % and the thickness of 2.0 mm respectively, ZnO networks possess preferable microwave absorption property, and the minimum reflection loss value is -30 dB at 14.4 GHz.

7. Acknowledgements

This work was supported by the National Basic Research Program of China (Grant No. 2007CB936201), the Funds for International Cooperation and Exchange (Grant Nos. 50620120439, 2006DFB51000), the Science Foundation (Grant Nos. 50772011, NCET-07-0066) and the Fundamental Research Funds for the Central Universities.

8. References

Cao, J. W.; Huang, Y. H.; Zhang, Y.; Liao, Q. L.; Deng, Z. Q. Research on electromagnetic wave absorbing properties of nano tetraleg ZnO. (2008). *Acta Physica Sinica,* 6, 3641-3645.

Chen, Y. J.; Cao, M. S.; Wang, T. H.; Wan, Q. (2004). Microwave absorption properties of the ZnO nanowire-polyester composites. *Appl. Phys. Lett.*, 84, 3367-3369.

Dai, Y.; Zhang, Y.; Li, Q. K.; Nan, C. W. (2002). Synthesis and optical properties of tetrapod-like zinc oxide nanorods. *Chem. Phy. Lett.,* 358, 83-86.

Dai, Y.; Zhang, Y.; Wang, Z. L. (2003). The octa-twin tetraleg ZnO nanostructures, *Solid State Commun.,* 126, 629–633

Fan, Z. J.; Luo, G. H.; Zhang, Z. F.; Zhou, L.; Wei, F. (2006). Electromagnetic and microwave absorbing properties of multi-walled carbon nanotubes/polymer composites. *Mater. Sci. Eng. B,* 132, 85-89.

Fang, X. Y.; Cao, M. S.; Shi, X. L.; Hou, Z. L.; Song, W. L.; Yuan, J.; (2010). Microwave responses and general model of nanotetraneedle ZnO: Integration of interface scattering, microcurrent, dielectric relaxation, and microantenna. *J. Appl. Phys.*, 107, 054304.

Fujii, M.; Iwanaga, H.; Ichihara, M.; Takeuchi, S. (1993). Structure of tetrapod-like ZnO crystals. *J. Cryst. Growth,* 128, 1095-1098.

Iijima, S. (1991). Helical microtubules of graphitic carbon. *Nature*, 354, 56-58.

Kimura, S.; Kato, T.; Hyodo, T.; Shimizu, Y.; Egashira, M. (2007). Electromagnetic wave absorption properties of carbonyl iron-ferrite/PMMA composites fabricated by hybridization method. *J. Magn. Magn. Mater.,* 312, 181-186.

Li, H. F.; Huang, Y. H.; Sun, G. B.; Yan, X. Q.; Yang, Y.; Wang, J.; Zhang, Y. (2010). Directed Growth and Microwave Absorption Property of Crossed ZnO Netlike Micro-/ Nanostructures. *J. Phys. Chem. C*, 114, 10088–10091.

Li, H. F.; Wang, J,; Huang, Y. H.; Yan, X. Q.; Qi, J. J.; Liu, J.; Zhang, Y. (2010). Microwave absorption properties of carbon nanotubes and tetrapod-shaped ZnO nanostructures composites. *Mater. Sci. Eng. B,* 175, 81-85

Sun, G. B.; Zhang, X. Q.; Cao, M. H.; Wei, B. Q.; Hu, C. W. (2009). Facile Synthesis, Characterization, and Microwave Absorbability of CoO Nanobelts and Submicrometer Spheres. *J. Phys. Chem. C,* 113, 6948-6954.

Wang, X. D.; Song, J. H.; Wang, Z. L. (2007). Nanowire and nanobelt arrays of zinc oxide from synthesis to properties and to novel devices. *J. Mater. Chem.*, 17, 711-720.

Wang, Z. L.; Kong, X. Y.; Zuo, J. M. (2003). Induced Growth of Asymmetric Nanocantilever Arrays on Polar Surfaces. *Phys. Rev. Lett.,* 91, 185502.

Wang, Z.L.; Song, J.H. (2006). Piezoelectric Nanogenerators Based on Zinc Oxide Nanowire Arrays. *Science,* 312, 242-246.

Yusoff, A. N.; Abdullah, M. H.; Ahmad, S. H.; Jusoh, S. F.; Mansor, A. A.; Hamid, S. A. A. (2002). Electromagnetic and absorption properties of some microwave absorbers. *J. Appl. Phys.,* 92, 876-882.

Zhang, L.; Zhu, H.; Song, Y.; Zhang, Y. M.; Huang, Y. (2008). The electromagnetic characteristics and absorbing properties of multi-walled carbon nanotubes filled with Er_2O_3 nanoparticles as microwave absorbers. *Mater.Sci.Eng.B*, 153. 78–82.

Zhao, D. L.; Li, X.; Shen, Z. M. (2008). Electromagnetic and microwave absorbing properties of multi-walled carbon nanotubes filled with Ag nanowires. *Mater. Sci. Eng. B,* 150, 105-110.

Zhao, D. L.; Shen, Z. M. (2008). Preparation and microwave absorption properties of carbon nanocoils. *Mater. Lett.,* 62, 3704-3706.

Zhou, Z.; Chu, L.; Tang, W.; Gu, L. (2003). Studies on the antistatic mechanism of tetrapod-shaped zinc oxide whisker. *J. Electrostatics,* 57, 347-354.

Zhu, J.; Peng, H. L.; Chan, C. K.; Jarausch, K.; Zhang, X. F.; Cui, Y. (2007). Hyperbranched Lead Selenide Nanowire Networks. *Nano Lett.,* 7, 1095-1099.

Zhuo, R. F.; Feng, H. T.; Chen, J. T.; Yan, D.; Feng, J. J.; Li, H. J.; Geng, B. S.; Cheng, S.; Xu; X. Y.; Yan, P. X. (2008). Multistep Synthesis, Growth Mechanism, Optical, and Microwave Absorption Properties of ZnO Dendritic Nanostructures. *J. Phys. Chem. C.*, 112, 11767.

Zhuo, R. F.; Qiao, L.; Feng, H. T.; Chen, J. T.; Yan, D.; Wu, Z. G.; Yan, P. X. (2008). Microwave absorption properties and the isotropic antenna mechanism of ZnO nanotrees. *J. Appl. Phys.*, 104, 094101.

Zou, Y. H.; Jiang, L. Y.; Wen, S. C.; Shu, W. X.; Qing, Y. J.; Tang, Z. X.; Luo, H. L.; Fan, D. Y. (2008). Enhancing and tuning absorption properties of microwave absorbing materials using metamaterials. *Appl. Phys. Lett.,* 93, 261115.

Zou, Y. H.; Liu, H. B.; Yang, L.; Chen, Z. Z. (2006). The influence of temperature on magnetic and microwave absorption properties of Fe/graphite oxide nanocomposites. *J. Magn. Magn. Mater.,* 302, 343-347.

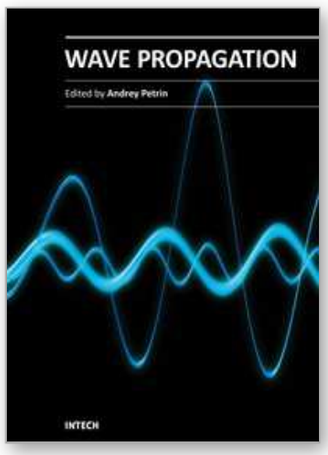

Wave Propagation
Edited by Dr. Andrey Petrin

ISBN 978-953-307-275-3
Hard cover, 570 pages
Publisher InTech
Published online 16, March, 2011
Published in print edition March, 2011

The book collects original and innovative research studies of the experienced and actively working scientists in the field of wave propagation which produced new methods in this area of research and obtained new and important results. Every chapter of this book is the result of the authors achieved in the particular field of research. The themes of the studies vary from investigation on modern applications such as metamaterials, photonic crystals and nanofocusing of light to the traditional engineering applications of electrodynamics such as antennas, waveguides and radar investigations.

How to reference
In order to correctly reference this scholarly work, feel free to copy and paste the following:

Yue Zhang, Yunhua Huang and Huifeng Li (2011). Electromagnetic Wave Absorption Properties of Nanoscaled ZnO, Wave Propagation, Dr. Andrey Petrin (Ed.), ISBN: 978-953-307-275-3, InTech, Available from: http://www.intechopen.com/books/wave-propagation/electromagnetic-wave-absorption-properties-of-nanoscaled-zno

INTECH
open science | open minds

InTech Europe
University Campus STeP Ri
Slavka Krautzeka 83/A
51000 Rijeka, Croatia
Phone: +385 (51) 770 447
Fax: +385 (51) 686 166
www.intechopen.com

InTech China
Unit 405, Office Block, Hotel Equatorial Shanghai
No.65, Yan An Road (West), Shanghai, 200040, China
中国上海市延安西路65号上海国际贵都大饭店办公楼405单元
Phone: +86-21-62489820
Fax: +86-21-62489821

IntechOpen